

Autonomous Underwater Simultaneous Localisation and Map Building

Stefan B. Williams, Paul Newman, Gamini Dissanayake, Hugh Durrant-Whyte

Australian Centre for Field Robotics

Department of Mechanical and Mechatronic Engineering

University of Sydney

NSW 2006, Australia

Abstract

In this paper we present results of the application of a Simultaneous Localisation and Map building (SLAM) algorithm to estimate the motion of a submersible vehicle. Scans obtained from an on-board sonar are processed to extract stable point features in the environment. These point features are then used to build up a map of the environment while simultaneously providing estimates of the vehicle location. Results are shown from deployment in a swimming pool at the University of Sydney as well as from field trials in a natural environment along Sydney's coast. This work represents the first instance of a deployable underwater implementation of the SLAM algorithm.

1 Introduction

Simultaneous Localisation and Map Building (SLAM) is the process of concurrently building up a feature based map of the environment and using this to obtain estimates of the location of the vehicle [2][3][4][5][9]. The robot typically starts at an unknown location with no a priori knowledge of landmark locations. From relative observations of landmarks, it simultaneously computes an estimate of vehicle location and an estimate of landmark locations. While continuing in motion, the robot builds a complete map of landmarks and uses these to provide continuous estimates of vehicle location.

Current work on undersea vehicles at the Australian Centre for Field Robotics concentrates on the development of terrain-aided navigation techniques, such as SLAM. Accurate position and attitude estimation and control methods use information from scanning sonar to complement a limited vehicle dynamic model and unobservable environmental disturbances. Key elements of this work include the development of sonar feature models, the tracking and use of these models in mapping and position estimation, and the development of low-speed platform models used in vehicle control.

Tests of these techniques are performed on a mid-size submersible robotic vehicle called Oberon designed and built at the Centre (see Figure 1). The vehicle is equipped with two scanning low frequency terrain-aiding sonars and a colour CCD camera, together with bathy-



Fig. 1. Oberon at Sea

ometric depth sensors and a fiber optic gyroscope [10]. This device is intended primarily as a research platform upon which to test novel sensing strategies and control methods. Autonomous navigation using the information provided by the vehicle's on-board sensors represents one of the ultimate goals of the project [7].

In this paper we present results of the application of Simultaneous Localisation and Map building to estimate the motion of the vehicle. This work represents the first instance of a deployable underwater implementation of the SLAM algorithm. Section 2 summarizes the stochastic mapping algorithm used for SLAM. Section 3 presents the feature extraction and data association techniques used to generate the observations for the filter. In Section 4 we describe a series of trials and show the results of applying this technique to data collected in the pool as well as in a natural terrain environment. Finally, Section 5 concludes the paper by summarizing the results and discussing future research topics as well as on-going work.

2 The Estimation Process

The localisation and map building process consists of a recursive, three-stage update procedure comprising prediction, observation and update steps using an Extended Kalman Filter (EKF). The state estimate $\hat{x}(k)$ is the augmented state vector consisting of the two dimensional pose of the vehicle $\hat{x}_v(k)$, made up of the position (x_v, y_v) and orientation ψ_v , together with the estimates of the positions of the N landmarks \hat{x}_i , $i = 1 \dots N$ [3].

Point landmarks are currently tracked in the map although the state formulation of the estimates can accommodate higher order features such as lines, curves and polylines.

2.1 Prediction

The prediction stage uses a model of the motion of the vehicle to update the predicted vehicle position $\hat{x}_v(k+1|k)$. As shown in equation 1, a simple linear velocity model is used to predict the position of the sub. The vehicle velocity V is assumed to be proportional to the mean lateral thruster setting. Given the small submerged inertia, relatively slow motion and large drag-coefficients induced by the open frame structure of the vehicle, this tends to be a reasonable model to use. This prediction equation can be stated more simply using the non-linear state update equation F_v .

$$\begin{aligned}\hat{x}_v(k+1|k) &= \hat{x}_v(k|k) + V\Delta T \cos(\hat{\psi}(k|k)) \\ \hat{y}_v(k+1|k) &= \hat{y}_v(k|k) + V\Delta T \sin(\hat{\psi}(k|k)) \\ \hat{\psi}_v(k+1|k) &= \hat{\psi}_v(k|k) + \Delta\psi\Delta T \\ \hat{x}_v(k+1|k) &= F_v(\hat{x}_v(k|k)), u_v(k|k))\end{aligned}\quad (1)$$

2.2 Observation

Observations are made using the SeaKing sonar. Point features are extracted from the sonar scans and are matched against existing features in the map. The feature matching algorithm will be described in more detail in Section 3. The observation consists of a relative distance and orientation from the vehicle to the feature.

2.3 Update

The innovation sequence consists of the difference between the predicted observation and the actual observations. If an observation is validated using the innovation gate, the state estimate is updated using the optimal gain matrix $W(k)$. This gain matrix provides a weighted sum of the prediction and observation and is computed using the innovation covariance and prediction covariance.

3 Feature Extraction

The development of autonomous map based navigation relies on the ability of the system to extract appropriate and reliable features with which to build its maps. Point features are identified from the sonar scans returned by the imaging sonar and are used to build up a map of the environment. These point features are easily identified and are selected to be stable over time.

Sonar targets are currently introduced into the environment in which the AUV will operate (see Figure 2). A prominent portion of the reef wall or a rocky outcropping might also be classified as a point feature. If the naturally occurring point features are stable they will

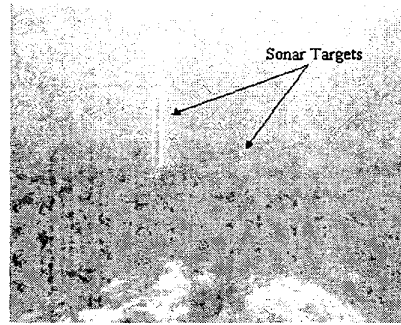


Fig. 2. An image captured from the submersible of one of the sonar targets deployed at the field test site.

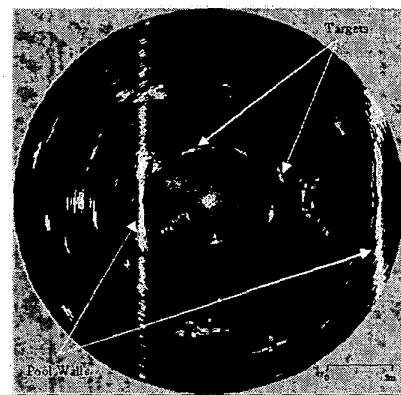


Fig. 3. Scan in the pool showing sonar targets

also be incorporated into the map. We are in the process of developing techniques to extract more complex natural features such as coral reefs and natural variations on the sea floor. This will allow the submersible to be deployed in a larger range of natural environments without the need to introduce artificial beacons.

The sonar targets produce strong sonar returns that can be characterised as point targets for the purposes of mapping (see Figure 3). The lighter sections in the scan indicate stronger intensity returns. As can be seen from the figure, the pool walls act as specular reflectors causing a considerable amount of additional sonar noise as well as multiple reflections that appear 'behind' the walls.

The extraction of point features from the sonar data is essentially a three stage process. The range to the principal return must first be identified in individual pings. This represents the range to the object that has produced the return. This is complicated by such issues as multiple and/or specular reflections, problems which we see in the pool but less so in a natural environment.

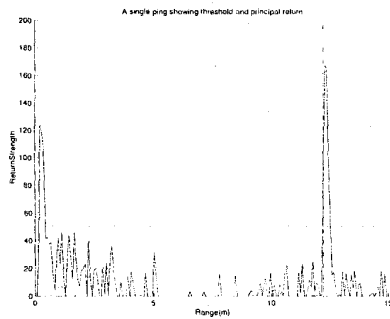


Fig. 4. A single SeaKing ping showing threshold and principal return. This ping is a reflection from one of the sonar targets. The dotted line indicates the threshold value while the dash-dot line marks the principal return.

The principal returns must then be grouped into clusters. Small, distinct clusters can be identified as point features and the range and bearing to the target estimated. Finally, the range and bearing information must be matched against existing features in the map.

3.1 Principal Returns

The data returned by the SeaKing sonar consists of the complete time history of each sonar ping in a discrete set of bins scaled over the desired range. The first task in extracting reliable features is to identify the principal return from the ping data. We consider the principal return to be the start of the maximum energy component of the signal above a certain noise threshold [8]. Figure 4 shows a single ping taken from a scan in the field. This return is a reflection from one of the sonar targets and the principal return is clearly visible. The return exhibits very good signal to noise ratio making the extraction of the principal returns relatively straightforward.

3.2 Identification of Point Features

The principal returns are then processed to find regions of constant depth within the scan that can be classified as point features. Sections of the scan are examined to find consecutive pings from which consistent principal return ranges are located. The principal returns are classified as a point feature if the width of the cluster is small enough to be characterised as a point feature and the region is spatially distinct with respect to other returns in the scan[8]. The bearing to the feature is computed using the centre of the distribution of principal returns. The range is taken to be the median range of the selected principal returns.

A scan taken in the field is shown in Figure 5. Three targets are clearly visible in the scan along with a section of the reef wall. Figure 6 shows the principal returns

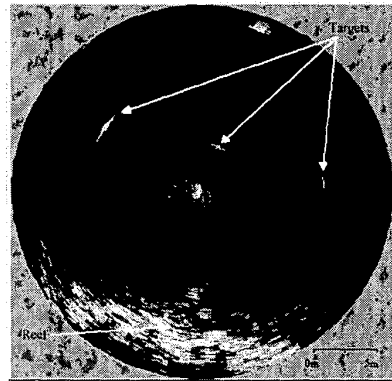


Fig. 5. Scan in the field showing sonar targets.

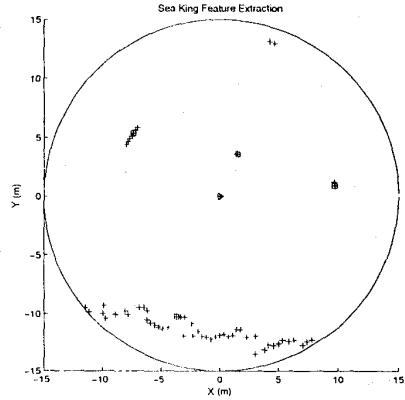


Fig. 6. This figure shows the principal returns (plus) and the extracted point features (squares) from the scan in figure 5.

selected from the scan along with the point features extracted by the algorithm. All three targets are correctly classified as point features. A prominent portion of the reef wall is also classified as a point feature.

3.3 Feature Matching

Once a point feature has been extracted from a scan, it must be matched against known targets in the environment. A two-step matching algorithm is used in order to reduce the number of targets that are added to the map (see Figure 7).

When a new range and bearing observation is received from the feature extraction process, the estimated position of the feature is computed using the current estimate of vehicle position. This position is then compared with the estimated positions of the features in the map using the Mahalanobis distance [3]. If the observation can be associated to a single feature the EKF is used to generate a new state estimate. An observation that

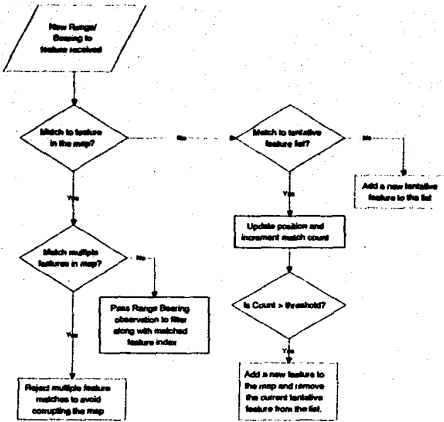


Fig. 7. The feature matching algorithm

can be associated with multiple targets is rejected since false observations can destroy the map's integrity.

If the observation does not match to any targets in the current map, it is compared against a list of tentative targets. Each tentative target maintains a counter indicating the number of associations that have been made with the feature as well as the last observed position of the feature. If a match is made, the counter is incremented and the observed position is updated. When the counter passes a threshold value, the feature is considered to be sufficiently stable and is added to the map. If the potential feature cannot be associated with any of the tentative features, a new tentative feature is added to the list.

4 Results

This section describes results from the deployment of the vehicle during testing in the swimming pool at the University of Sydney and in a natural terrain environment along Sydney's coast. We show that the filter estimates appear to be consistent by comparing the estimates to ground truth in the pool and by monitoring the innovation sequences in the field.

4.1 Swimming Pool trials

During tests in the pool at the University of Sydney, six sonar targets form a circle roughly 6m in diameter in the area in which the sub is operating. The submersible starts to the left of the target cluster and is driven in a straight line perpendicular to the pool walls over a distance of approximately 5m. The sub is then driven backwards over the same distance and returns to the initial position. A PID controller maintains the heading of the sub using feedback from a fiber optic gyro. During the short duration of the trials, the accumulated drift in the gyro orientation estimate is considered negligible.

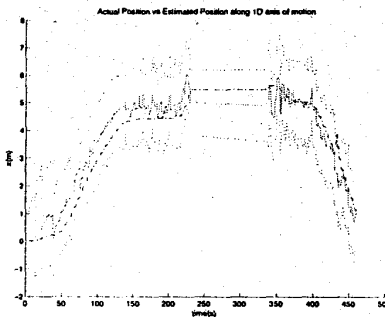


Fig. 8. Position of the robot in the pool along the 1D axis of motion. The estimate is the solid line, the true position the dash-dot line while the error bounds are shown as the dotted lines.

Forward thrust is achieved by adding a common voltage to each thruster amplifier control signal [10].

In order to determine the true position of the sub in the pool, we use the distance to the pool walls measured with the sonar. The walls are clearly evident in the scans taken in the pool giving us a good approximation of the actual position of the sub.

Figure 8 shows the position estimate along the axis perpendicular to one of the pool walls generated by SLAM during one of the runs in the pool. These results show that the robot is able to successfully determine its position relative to the walls of the pool despite the effect of the tether, which tends to dominate the dynamics of the vehicle at low speeds. With the low thruster setting, the AUV stops after it has traversed approximately 4.5m, with the catenary created by the deployed tether overcoming the forward thrust created by the vehicle's thrusters. The sub currently has no full inertial unit but is still able to detect the fact that it has stopped using observations from its feature map.

The error in the X position relative to the pool walls is plotted along with the 95% confidence bounds in Figure 9. While the estimated error bounds are conservative, this allows the optimal estimator to account for environmental disturbances in the field such as current and the forces exerted by the tether catenary.

In order to test the filter consistency, the innovation sequences can be checked against the innovation covariance estimates. This is the only method available to monitor on-line filter performance when ground truth is unavailable. As can be seen in Figure 10, the innovation sequences for range and bearing are consistent.

We can also plot the error in the estimated position of the beacons against their respective 95% confidence bounds. This is shown in Figure 11 for Beacon 2 which was seen from the start of the run and Figure 12 for

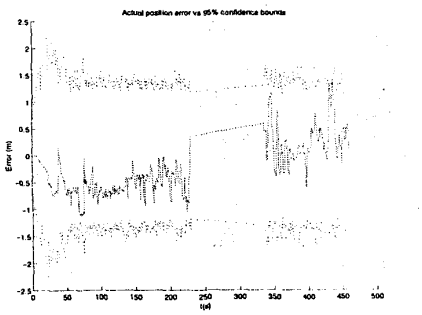


Fig. 9. The 95% confidence bounds computed using the covariance estimate for the error in the X estimate compared to the actual error relative to the pool walls.

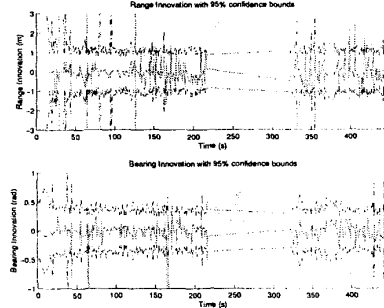


Fig. 10. The range and bearing innovation sequences plotted against their 95% confidence bounds. The innovation is plotted as a solid line while the confidence bounds are the dash-dot lines.

Beacon 4 which is only incorporated into the map after the first minute.

The final map generated by the SLAM algorithm is plotted in Figure 13. The true position of the sonar targets is shown and the associated map features can clearly be seen in the final map estimates. A number of point features have also been identified along the pool wall to the left of the image. The estimated path of the submersible is shown along with the covariance ellipses describing the confidence in the estimate. It is clear that the covariance remains fairly constant throughout the run.

4.2 Field trials

We have also tested the SLAM algorithms during deployment in a natural environment off the coast of Sydney. The sub was deployed in a natural inlet with the sonar targets positioned in a straight line in intervals of 10m. Since there is currently no absolute position sensor on the vehicle, we cannot measure the performance of the positioning filter against ground truth at this time.

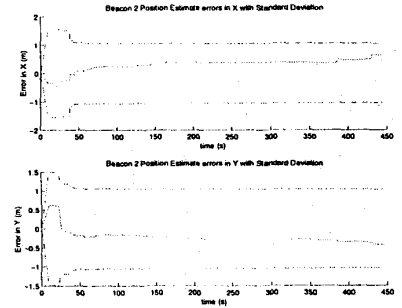


Fig. 11. The Error in the estimated X and Y positions for Beacon 2 along with the 95% confidence bounds. This shows that the beacon location estimate is consistent.

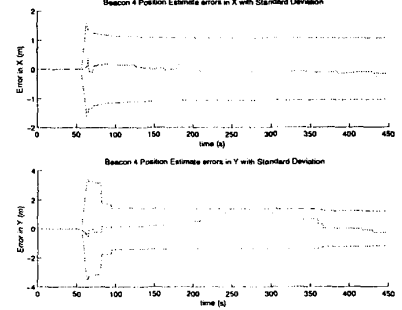


Fig. 12. The Error in the estimated X and Y positions for Beacon 4 along with the 95% confidence bounds. This shows that the beacon location estimate is consistent.

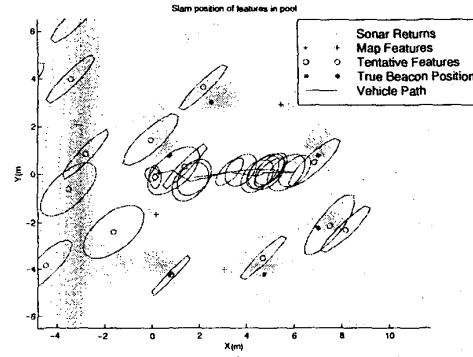


Fig. 13. Path of the robot shown against the final map of the environment. The estimated position of the features are shown as circles with the covariance ellipses showing their 95% confidence bounds. The true positions are plotted as '**'. Tentative targets that have not yet been added to the map are shown as '+'. The robot starts at (0,0) and traverses approximately 5m in the X direction before returning along the same path in the reverse direction.

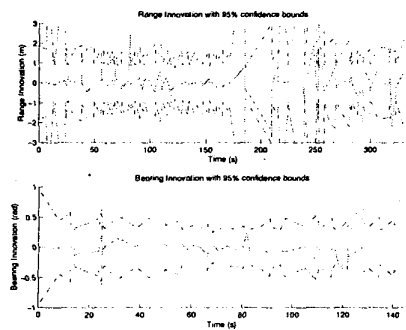


Fig. 14. The range and bearing innovation sequences plotted against their 95% confidence bounds. The innovation is plotted as a solid line while the confidence bounds are the dash-dot lines.

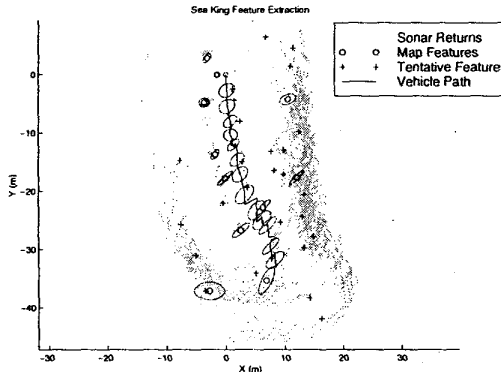


Fig. 15. Path of robot shown against final map of the environment. The estimated position of the features are shown as circles with the covariance ellipses showing their 95% confidence bounds. Tentative targets that have not yet been added to the map are shown as '+'. The series of tentative targets to the right of the image occur from the reef wall. The natural point features tend not to be very stable, though, and are thus not incorporated into the map.

We can, however, monitor the innovation sequence to check the consistency of the estimates. Figure 14 shows that the innovation sequences appear to be within the covariance bounds computed by the algorithm.

The plot of the final map shown in Figure 15 clearly shows the position of the sonar feature targets along with a number of tentative targets. Some of the tentative targets are from the reef wall while others come from returns off of the tether. These returns are typically not very stable and therefore do not get incorporated into the SLAM map. The sonar principal returns have been plotted relative to the estimated position of the vehicle. The reef wall to the right of the vehicle and the end of the inlet are clearly visible.

5 Summary and Conclusions

We have been testing the Oberon system in a number of locations. At present, we have shown that SLAM is practically feasible in both a swimming pool at the University of Sydney and in a natural terrain environment on Sydney's shore-line.

The focus of recent work has been on the development of criteria for feature selection as a function of the geometric distribution of features in an environment as well as based on the current mission being run. Incorporation of the SLAM architecture into the mission planning loop will allow decisions concerning sensing strategies to be made in light of the desired mission objectives.

Another outstanding issue is that of map management. As the number of calculations required to maintain the state covariance estimates increases with the square of the number of beacons in the map, criteria for eliminating features from the map as well as for partitioning the map into submaps becomes important. This is especially true for longer missions in which the number of available landmarks is potentially quite large.

References

- [1] Bauer R, Rencken WD. "Sonar feature based exploration". Proceedings. 1995 IEEE/RSJ International Conference on Intelligent Robots and Systems. pp.148-53 vol.1. Los Alamitos, CA, USA, 1995
- [2] Castellanos JA, Montiel JMM, Neira J, Tardos JD. "Sensor Influence in the Performance of Simultaneous Mobile Robot Localization and Map Building". 6th International Symposium on Experimental Robotics. pp 203-212, Sydney, NSW, Australia, 1999
- [3] Dissanayake MWMG, Newman P, Durrant-Whyte HF, Clark S, Csorba M. "An Experimental and Theoretical Investigation into Simultaneous Localisation and Map Building". 6th International Symposium on Experimental Robotics. pp 171-180, Sydney, NSW, Australia, 1999
- [4] Feder HJS, Leonard JJ, Smith CM. "Adaptive sensing for terrain aided navigation". IEEE Oceanic Engineering Society-OCEANS'98. pp.336-41 vol.1. New York, NY, USA, 1998
- [5] Leonard JJ, Durrant-Whyte HF, "Simultaneous Map Building and Localisation for an Autonomous Mobile Robot", IEEE/RSJ International Workshop on Intelligent Robots and Systems IROS '91, pp.1442-1447, New York, NY, USA, 1991
- [6] Leonard JJ, Carpenter RN, Feder HJS, "Stochastic Mapping Using Forward Look Sonar", FSR '99 International Conference on Field and Service Robotics , pp.69-74, Pittsburg, PA, USA 1999
- [7] Newman P. and Durrant-Whyte HF, "Toward Terrain-Aided Navigation of a Subsea Vehicle", FSR'97 International Conference on Field and Service Robotics, pp.244-248, Canberra, Australia, 1997.
- [8] Newman P., "On The Structure and Solution of the Simultaneous Localisation and Map Building Problem", D.Phil Thesis, University of Sydney, 1999
- [9] Rencken WD. "Concurrent localisation and map building for mobile robots using ultrasonic sensors". Proceedings of the 1993 IEEE/RSJ International Conference on Intelligent Robots and Systems, pp.2192-7 vol.3. New York, NY, USA, 1993
- [10] Williams S, Newman P, Majumder S, Rosenblatt J, Durrant-Whyte H, "Autonomous Transect Surveying of the Great Barrier Reef", Australian Conference on Robotics and Automation (ACRA '99), Brisbane, QLD, 1999.